IJISET - International Journal of Innovative Science, Engineering & Technology, Vol. 4 Issue 8, August 2017
ISSN (Online) 2348 – 7968 | Impact Factor (2016) – 5.264
www.ijiset.com

"Polymer-multiwall carbon nanotube" nanocoatings on macroporous silicon matrix

Liudmyla Karachevtseva[1,2], Mykola Kartel[1,3], Wang Bo[1], Yurii Sementsov[1,3], Vyacheslav Trachevskiy[1], Oleg Lytvynenko[2] and Volodymyr Onyshchenko[2]

[1]Ningbo University of Technology, Ningbo, 315016, China

[2]V. Lashkaryov Institute of Semiconductor Physics NASU, Kyiv, 03028, Ukraine

[3]O. Chuiko Institute of Surface Chemistry NASU, Kyiv, 03164, Ukraine

Abstract

Carbon nanotubes are among the most anisotropic materials known and have extremely high values of Young's modulus. The possibilities to enhance the properties of nanostructured surfaces were demonstrated on "polymer-multiwall carbon nanotube" composites and composite nanocoatings on macroporous silicon structures. Influence of sp^3 hybridization bonds on polymer crystallization and strengthening was investigated in composite films of polypropylene and polyamide with carbon multiwall nanotubes. It was established that the effective way to improve the strength properties of "polymer-multiwall carbon nanotube" composites is the composite crystallization and sp^3 C-C tetrahedrons organization between nanotubes supported by $\gamma_\omega(CH)$ and $\gamma_\omega(CH_2)$ vibrations in the intrinsic electric field. The effects of blooming, photoluminescence increase and surface bond passivation by nanocoatings of "polymer-multiwall carbon nanotube" on macroporous silicon structures were evaluated.

Keywords: *Polymer Composites, Multiwall Carbon Nanotubes, Macroporous Silicon Matrix.*

1. Introduction

Multiwall carbon nanotubes are among the most anisotropic materials known and have extremely high values of Young's modulus [1]. Carbon nanotube aspect ratio of length to diameter is more than 10^3; this distinguishes it from other nanoparticles. New composites with carbon nanotubes (CNTs) as additives were studied intensively during the last decade. Composites are characterized by extremely high specific strength properties [2], electrical and thermal conductivity [3]. The presence of CNT in the matrix improves the composite biocompatibility [4]. CNTs exhibit both semiconducting and metallic behavior depending on their chirality [5]. The researchers have successfully demonstrated field-effect transistors based on semiconducting CNTs [6]. Metallic CNTs have been considered as a potential solution for on-chip interconnects with a current density well above 10^6 A/cm^2 [7]. The connection of CNTs to silicon has been realized, using polyethyleneimine (PEI) as a binding material between them [8]. Chemical hydrogen bonding and electrostatic interaction between PEI, CNTs, and silicon effectively connect CNTs to silicon. Electric transport at this junction shows a tunneling behavior, which verifies PEI as a molecular link between CNT tips and silicon.

Last years structures of macroporous silicon became a promising material for development of 2D photonic structures with required geometry and large effective surface [9]. This determines the optical and electro-optical characteristics of macroporous silicon structures [10-12]. In view of a potential barrier on macropore surface, one should take into account recharging of the local surface centers at energies below that of the indirect interband transition. Macroporous silicon has found application in sensors based on measurements of optical, electric, photovoltaic and photoluminescence characteristics. Thus, macroporous silicon-based optical biosensors were designed to detect low concentrations of DNA [13]. The capacitive humidity sensors [14], gas and biosensors of CMOS-compatible manufacturing, solar cells with efficiency up to 13% [15] and coating with less than 0.1% reflection have been developed [16].

In this paper, the opportunities to enhance the properties of nanostructured surfaces are demonstrated on "polymer-multiwall carbon nanotube" composites and composite nanocoatings on macroporous silicon structures. Influence of sp^3 hybridization bonds on polymer strengthening is investigated in composites of PEI, polypropylene and polyamide with multiwall carbon nanotubes. The effects of blooming, photoluminescence increase and surface bond passivation by nanocoatings of "PEI-multiwall carbon nanotubes" on macroporous silicon structures are evaluated.

2. Materials and Methods

Carbon high purity multiwall nanotubes (CNTs) of 2 μm length and 20 nm diameter (Fig. 1a) were obtained by catalytic pyrolysis of unsaturated

hydrocarbons [17]. Nanoparticle morphology was investigated by the atomic force microscopy (AFM, NanoScope IIIa Dimension 3000TM, Advance Surface Microscopy Inc.). The composites were made of PEI, polypropylene and polyamide filled by a mixture of CNTs with the polymer powder and dried; the samples were formed by hot pressing.

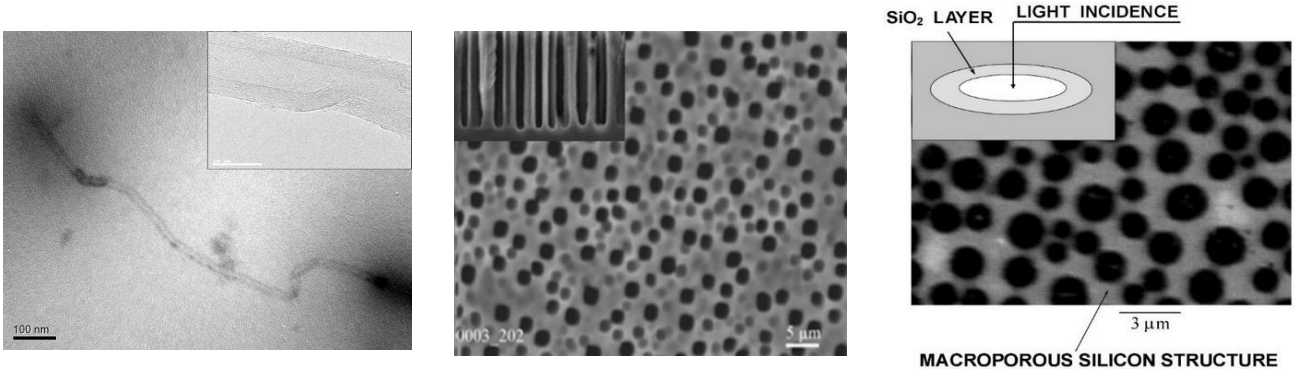

Fig. 1 a) Morphology of multiwall nanotubes according to the AFM data; b) A fragment of a macroporous silicon structure with arbitrary distribution of macropores; c) Direction of light incidence on the sample (along the main axis of cylindrical macropore).

Compression and tension tests of the polymeric materials and their composites were performed using tensile machine 2167-R50 with automatic recording of the deformation diagram. Thin polymeric films (100-150 μm thick) without and with CNTs were prepared out using Thermo HYDROPRESS.

Macroporous silicon structures with arbitrary distribution of macropores (Fig. 1b) were made of *n*-silicon wafers (the [100] orientation, the electron concentration $n_0 = 10^{15}$ cm^{-3}). We used the technique of electrochemical etching at illumination of the backside of a silicon substrate (thickness H = 520 μm) [18, 19]. The initial samples are complex micropore-macropore silicon structures consisting of 150 nm micropore layers on macropore walls. An additional anisotropic etching in 10% solution of KOH was used to remove the microporous layers from macropore walls. According to the results of optical microscopy (Nu, Carl Zeiss Jena, Germany), macropores with depth h_p = 40-120 μm, diameter D_p = 2-5 μm and concentration $N_p = (1\text{-}6)\cdot 10^6$ cm^{-2} were formed. The oxide layers (thickness of 20 nm) were formed on macroporous silicon samples in dry oxygen for 40-60 min at a temperature of 1050 °C. The oxide thickness was measured using ellipsometry with 0.2 nm accuracy. The nanocoatings "polymer-multiwall carbon nanotubes" were obtained from a colloidal solution of PEI with CNT onto (1) single crystalline Si, (2) macroporous Si, (3) oxidized macroporous Si, and (4) macroporous Si with microporous Si layer.

The chemical states on the surface of macroporous silicon structures with nanocoatings were identified by IR absorption spectra using a PerkinElmer Spectrum BXII IR Fourier spectrometer in the spectral range of 300-8000 cm^{-1}. The optical absorption spectra were measured at normal incidence of IR radiation on the sample (along the main axis of cylindrical macropores, Fig. 1c). Raman spectra of macroporous silicon structures with nanocoatings of PEI with multiwall carbon nanotubes were measured using a Horiba Jobin-Yvon T64000 spectrometer. The photoluminescence spectra of the nanocoatings on macroporous silicon samples were obtained in the 1.8-3.3 eV range of photon energy. The excitation radiation with photon energy of 0.34 eV falls on the sample through an optical fiber; photoluminescence emission of the test sample falls on the sensor and optical fiber through a slit (width of 2.5 nm). The angle between the excitation radiation and photoluminescence emission is 5º. The IR absorption, Raman and photoluminescence spectra measurements were carried out in air at room temperature.

3. Results and Discussion

3.1. "Polymer-carbon multiwall nanotube" composites

Intensive peaks of sp^3-hybrid orbitals (D), sp^2-hybrid orbitals (G), 2D and CH_2 bonds were measured in the IR spectra (Fig. 2a, curve 1) and Raman spectra (Fig. 2a, curve 2) of multiwall carbon nanotubes.

Fig. 2b shows the absorption spectra of PEI (curve 1), the composite "PEI-carbon nanotubes" (curve 2) and the ratio of spectra 1 and 2 (curve 3). After formation of the PEI-CNT composite intensive absorption maxima were measured in area of the sp^3 hybridization (D) bonds at the frequency of N-H(1) oscillations in the primary amino groups of PEIs and in area of the sp^2 hybridization (G) bonds for the N-H(2) oscillation frequencies in secondary amino groups of PEIs.

Fig. 3a shows IR absorption spectra of polyamide (curve 1), "polyamide-carbon nanotubes" composite (curve 2) and the ratio of the curves 1 and 2 (curve 3).

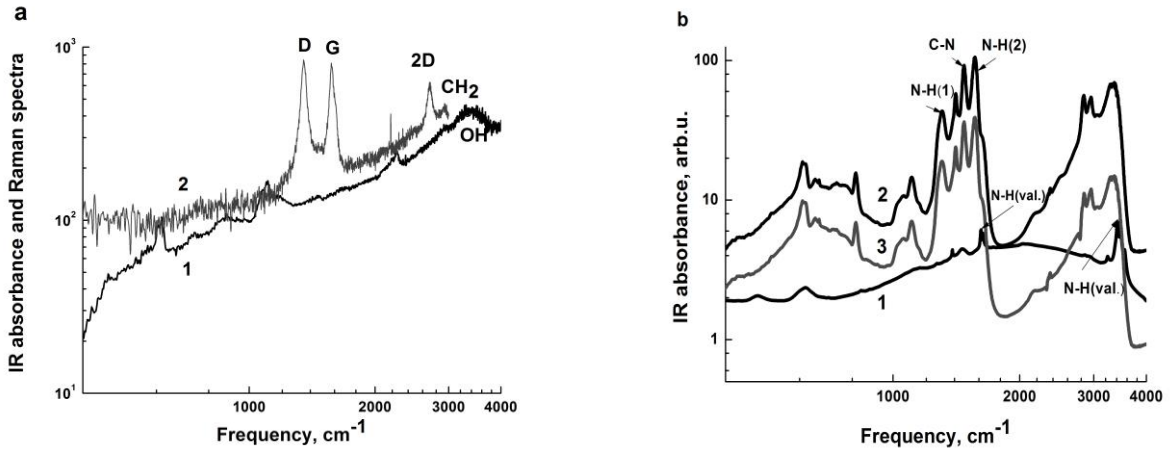

Fig. 2 a) IR absorption (1) and Raman (2) spectra of multiwall carbon nanotubes; b) IR absorption spectra of PEI (1), "PEI-CNT" composite (2) and its relation (3).

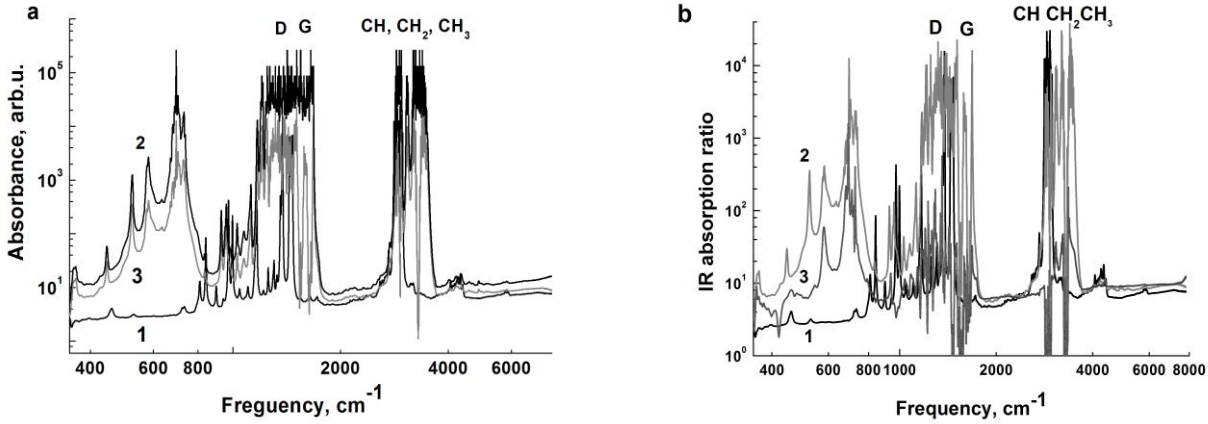

Fig. 3 a) IR absorption spectra: 1 – polyamide-6, 2 – "polyamide-carbon nanotubes" composite and 3 – the ratio of the curves 1 and 2; b) Ratio of IR absorption spectra of "composite/polymer": 1 – polypropylene, 2 – polyamide-6, 3 – polyamide-12.

Fig. 3b presents the ratio of IR absorption spectra of "composite/polymer" for films of polypropylene (PP) – curve 1, polyamide-6 (PA6) – curve 2) and polyamide-12 (PA12) – curve 3. After adding CNTs to polymers (concentration of 0.25%), IR absorption of "composite/polymer" films exceeds that of polymer films essentially. Higher C-C fluctuations, CH, CH_2 and CH_3 bond absorption correspond to higher absorption of composites at the frequencies of sp^3 hybridization bonds. Table 1 shows type and frequency of bonds for the IR absorption growth at frequencies of sp^3 hybridization after adding carbon nanotubes to polymers. Thus, higher absorption of composites at the frequencies of sp^3 hybridization bonds is due to $\gamma_\omega(CH)$ and $\gamma_\omega(CH_2)$ vibrations (Table 1).

IR absorption by sp^3 hybridization bonds (D) in composites of polymers with multiwall carbon nanotubes has maxima (Fig. 4) at its dependencies on CNT content. Thus, the maxima correspond to fixed distance between nanotubes.

Table 1: Types of bonds for IR absorption growth at frequencies of sp^2 and sp^3 hybridization after adding to polymers carbon nanotubes

PP		PA6		PA12	
Type of bonds	Frequency, cm^{-1}	Type of bonds	Frequency, cm^{-1}	Type of bonds	Frequency, cm^{-1}
$\gamma_\omega(CH)$	1360	$\gamma_\omega(CH_2)$	1319, 1406	$\gamma_\omega(CH_2)$	1357

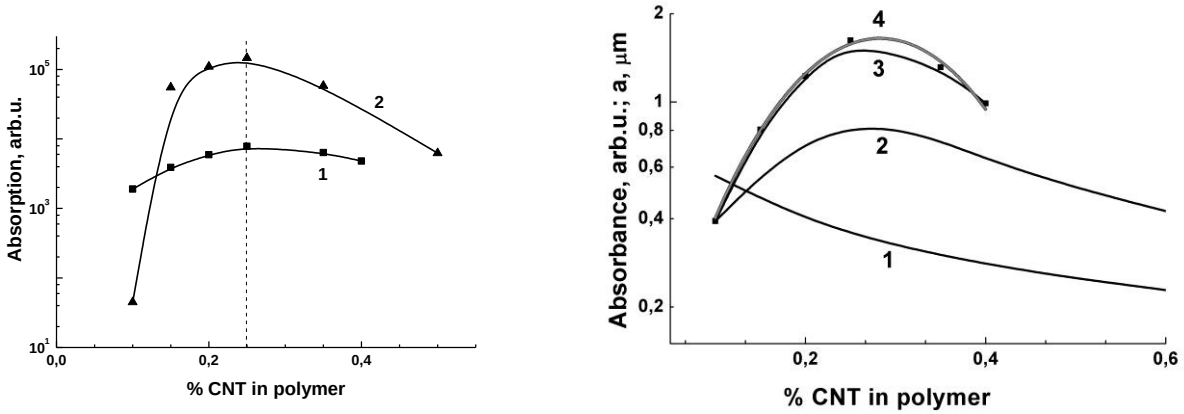

Fig. 4. IR absorption by sp^3 hybridization bonds (D) in composites based on polypropylene (1) and polyamide-6 (2) vs CNT content in polymer.

Fig. 5. Calculated dependences of average distance *a* between CNT (1), geometric approximation (2) – characteristic volume around CNT; experimental dependence from Fig. 4 of the IR absorption peak of sp^3 hybridization of "polypropylene – CNTs" composite (3) and its approximation (4) on CNT content.

Distance between nanotubes in composites depends on the concentration of CNT (N_{CNT}), its content (% CNT) and the nanotube volume (V_{CNT}):

$$a = (N_{CNT})^{1/2} = (\%\ \mathrm{CNT}/100V_{CNT})^{1/2} \qquad (1)$$

The IR absorption maximum for sp^3 hybridization bonds (D) of composites (Fig. 4) corresponds to the average distance $a = 0.35$ μm between the cylindrical CNT (diameter of 20 nm, length of 2 μm). This maximum can be explained by the geometric factor - characteristic volume around the cylindrical CNT at a distance of $a_m/2$ from nanotubes. As $a > a_m$, the characteristic volume around CNT increases due to increasing of the content of CNT (% CNT, N_{CNT}), IR absorption increases too. The characteristic volume around CNT and IR absorption decreases with CNT content at $a < a_m$,

Figure 5 shows the calculated (according to Eq. (1)) dependences of average distance *a* between CNT (curve 1), geometric approximation (curve 2, characteristic volume around CNT), experimental dependence from Fig. 4 of the IR absorption peak of sp^3 hybridization of "polypropylene-CNTs" composite (curve 3) on CNT content. The obtained geometric approximation (Fig. 5, curve 2) explains only qualitatively the experimental dependence of IR absorption peak in bonds sp^3 hybridization (D) of "polypropylene-carbon nanotube" composite on the CNT content. This relationship is more nonlinear and has the form of a 1D Gaussian curve (Fig. 5, curve 4), which corresponds to the diffusion equation in the electric field. The length $a = 0.35$ μm between cylindrical CNT corresponds to the distance between nanotubes $w = (a_m - d)/2 = 0.17$ μm for maximum of IR absorption. The electric field between the nanotubes and polymer matrix has a space charge region (SCR) width *w* (Fig. 6).

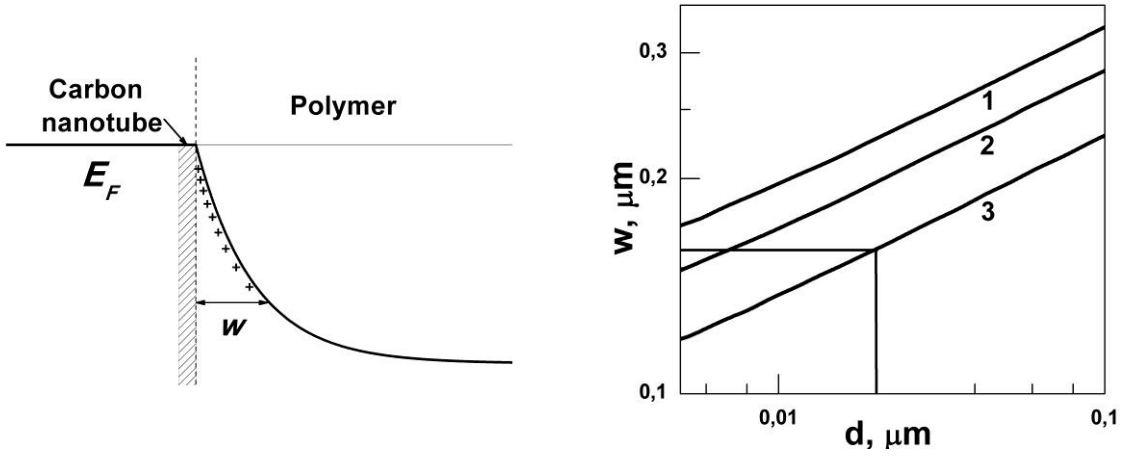

Fig. 6 Band bending and SCR width *w* at the "polymer - CNTs" boundary.

Fig. 7 Dependence of SCR width *w* around cylindrical nanotubes on its diameter for surface potential *Ys*: 1 – -12 *kT*; 2 – -8 *kT*; 3 – 4 *kT*.

IJISET - International Journal of Innovative Science, Engineering & Technology, Vol. 4 Issue 8, August 2017
ISSN (Online) 2348 – 7968 | Impact Factor (2016) – 5.264
www.ijiset.com

We used the Poisson equation in a cylindrical coordinate system to calculate the SCR width (Fig. 6) around a cylindrical nanotube:

$$\frac{1}{\mathbf{r}}\frac{\partial}{\partial \mathbf{r}}\left(\mathbf{r}\frac{\partial Y}{\partial \mathbf{r}}\right) = -\frac{\rho_q}{\varepsilon\varepsilon_0}\frac{e}{kT}\ , \qquad (2)$$

where r is the radius vector, ρ_q is the charge density. We used the boundary conditions for the area of the SCR width w for a cylindrical nanotube diameter d: $E(d/2 + w) = 0$, $Y(d/2 + w) = 0$, $Y(d/2) = Y_S$, where E is the electric field strength, Y_S - the value of the potential on the surface of the nanotube.
Integrating Eq. (2) and using the above boundary conditions, we obtained the equation [20]:

$$\frac{16\varepsilon\varepsilon_0 Y_S w}{eq_V d^2} - 1 + \left(1+\frac{2w}{d}\right)^2\left(1-2\ln\left(1+\frac{2w}{d}\right)\right) = 0 \qquad (3)$$

Fig. 7 shows dependences of the size of the space charge region of cylindrical nanotubes calculated from Eq. (3) on their diameter at various values of the surface potential. It is shown in Fig. 7 that the SCR width w decreases with the diameter of nanotubes decrease. Surface potential $Y_S = -4kT$ (106 mV) and electric field intensity $E = Y_S/w = 6.3\cdot10^3$ V/cm corresponds to $w = 0.17$ μm for cylindrical CNT (diameter of 20 nm, length of 2 μm) maximum at IR absorption peak for bonds of sp^3 hybridization (D).

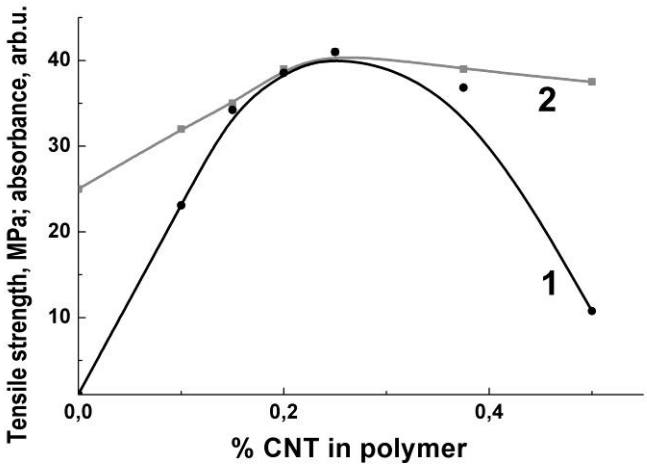

Fig. 8 Experimental dependence of the IR absorption peak of sp^3 hybridization (1) and tensile strength of "polyamyde-6-CNT" composite (2) on CNT concentration.

Carbon nanotubes are divided into two main groups: the molecular associated nanotubes linked through weak interactions, van der Waals forces, and nanotubes with additional strong covalent sp^3 type C-C bonding [8]. Thus, one of the way to improve the strength properties of "polymer-CNT" composites is the composite crystallization and sp^3 C-C tetrahedrons organization between nanotubes due to $\gamma_\omega(CH)$ and $\gamma_\omega(CH_2)$ vibrations (Table 1) in the intrinsic electric field. Really, the profile analysis of X-ray reflexes confirmed high crystallinity degree of investigated "polymer-CNT" composites - from 72% to 85% [21]. Crystalline polymers demonstrate high tensile strength. Experimental dependences of the IR absorption peak of sp^3 hybridization (Fig. 8, curve 1) and tensile strength of "polyamyde-6-CNT" composite (Fig. 8, curve 2) have the same peak at CNTs content of 0.25%. Tensile strength of PA6–CNT system with CNTs content of 0.25% is 30-40 MPa (Fig. 8).

3.2. "Polymer-carbon multiwall nanotube" nanocoatings on macroporous silicon matrix.

Fig. 9a shows IR (curve 1) and Raman (curve 2) spectra of macroporous silicon structures with "PEI-CNT" nanocoatings. The peaks of one-phonon in Si (305 cm^{-1}), two-phonon in Si (514 cm^{-1}), transverse acoustical phonon in Si (TA), sp^2- and sp^3-hybrid orbitals, twice carbon sp^3-hybrid orbitals (2D) and CH_2 bonds were measured in Raman spectra. The maximal Raman shift was measured for macroporous silicon with microporous silicon layer, with similar peaks of sp^2- and sp^3-hybrid orbitals and CH_2 bonds. Figure 9b shows the IR absorption spectra of macroporous silicon structures with "PEI-CNT" nanocoatings. The IR absorption spectra have the similar peak frequencies of surface states. High IR absorption was measured on macroporous silicon with microporous silicon layer (Fig.9b, curve 4). The IR absorption for substrates of oxidized macroporous silicon and macroporous silicon with c (Fig.9b. curves 2, 3) is lower and comparable.

Macroporous silicon without nanocoatings has depleted surface band banding (Fig. 10a).Thus, the PEI nanocoatings with carbon multiwall nanotubes increase surface depletion [12] and IR absorption of macroporous silicon without nanocoatings and decrease surface accumulation [10, 11] for SiO_2 coatings and microporous silicon layer.

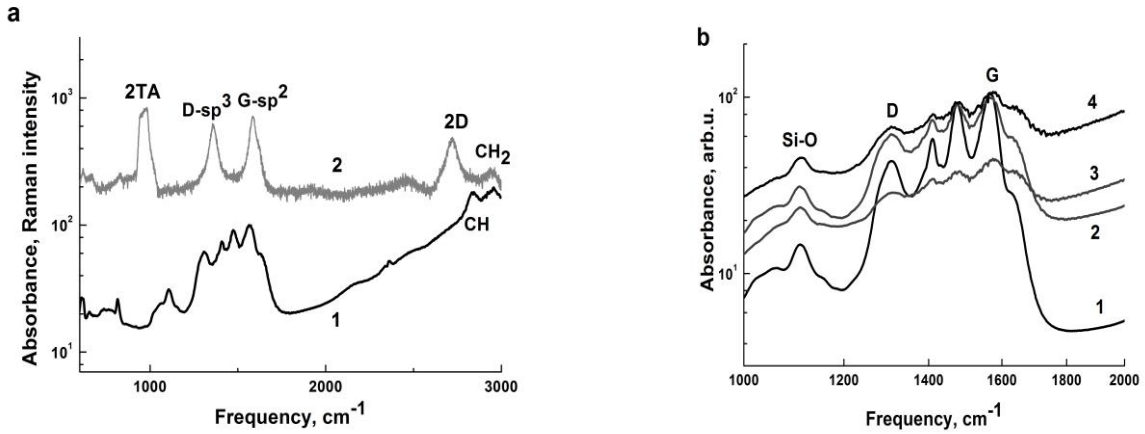

Fig. 9 a) IR (1) and Raman (2) spectra of macroporous silicon structure with "PEI-CNT" nanocoatings;
b) IR absorption spectra of silicon structures with "PEI-CNTs" nanocoatings: 1 – silicon single crystal, 2 – macroporous silicon, 3 – oxidized macroporous silicon, 4 – macroporous silicon with microporous layer.

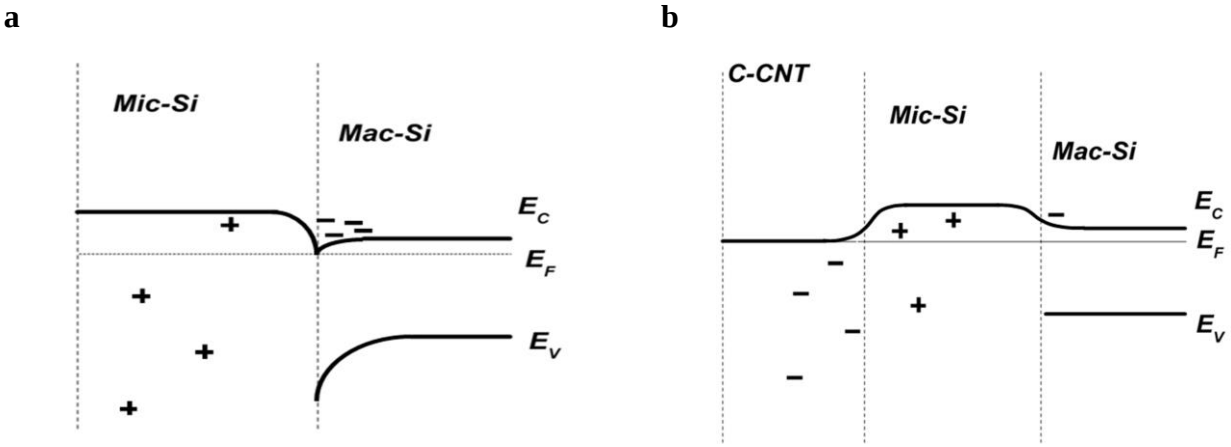

Fig. 10 a) Accumulation band bending of macroporous silicon with microporous Si; b) depleted band bending of macroporous silicon with microporous Si and "PEI-CNT" nanocoating.

Fig. 11a shows IR absorption spectra of macroporous silicon with microporous layer (curve 1). High oscillations of IR absorption were explained by the resonance electron scattering and Wannier–Stark effect realization [10, 11] on the accumulation surface of macroporous silicon matrix. The model [22, 23] of the resonance electron scattering on impurity states in an electric field of "silicon–nanocoating" heterojunction on macropore surface and realization of the Wannier–Stark effect on randomly distributed surface bonds were confirmed. In this case, the Wannier–Stark effect was measured due to a large-time electron scattering as compared with the period of its oscillations in the strong electric field of "silicon-nanocoating" interface. The "PEI-CNT" nanocoatings reduce IR absorption of macroporous Si with microporous Si (Fig. 11a) layer by 2-3 orders of magnitude (blooming effect up to frequencies of CH bond absorption) due to strong change of band bending on the macropore surface from accumulation one to flat or depleted band bending (Fig. 10b). It is due to carbon nanotubes in PEI and high concentration of hydrogen atoms [10] in the microporous layer. Thus, the electron charge of nanotubes neutralized the positive hydrogen bonds. Fig. 11b shows photoluminescence spectra (the photon excitation energy of 0.34 eV) of PEI with carbon nanotubes on macroporous silicon with microporous layer (1), on macroporous silicon (2), and on silicon single crystal (3). The photoluminescence intensity of PEI with multiwall carbon nanotubes is maximal for substrate of macroporous silicon with microporous silicon layer (Fig. 11b, curve 1). The photo-luminescence of polymer is determined by the exciton generation and electron-hole radiative

recombination [24]. The photoluminescence intensity of PEI with carbon multiwall nanotubes on macroporous silicon with microporous layer is 5.6 times higher than that of PEI with CNT on single crystalline silicon in the photon energy range of 2.2-2.7 eV. It is due to decrease of the proton non-radiative recombination on boundary nanocoating "PEI-CNT" and microporous layer (Fig. 10b) layer with positive charge of hydrogen atoms.

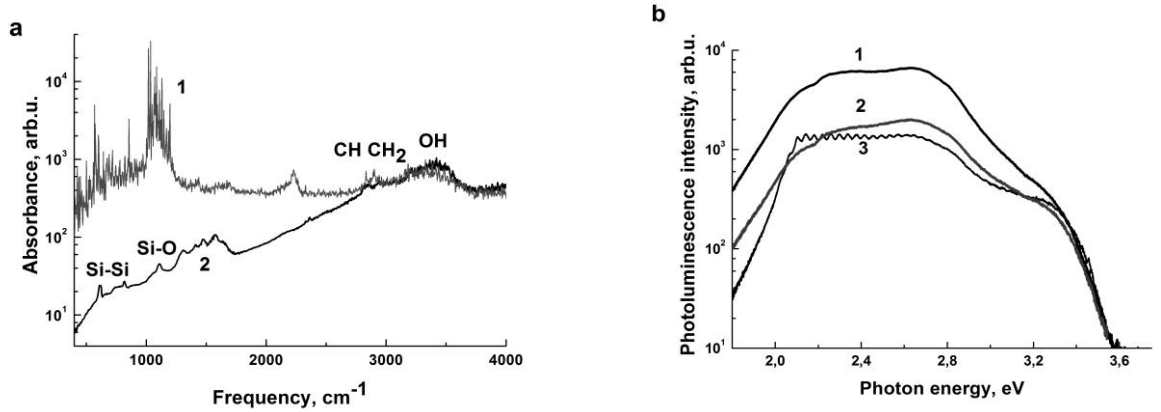

Fig. 11 a) IR absorption spectra of macroporous silicon with microporous layer without (1) and with (2) "PEI-CNT" nanocoatings. The "PEI-CNT" nanocoatings reduce IR absorption of macroporous Si with microporous Si layer by 2-3 orders of magnitude (the blooming effect);
b) photoluminescence spectra of PEI with multiwall carbon tubes on macroporous silicon with microporous layer (1), on macroporous silicon (2), and on silicon single crystal (3).

4. Conclusions

Carbon nanotubes are among the most anisotropic materials known and have extremely high values of Young's modulus. The possibilities to enhance the properties of nanostructured surfaces were demonstrated on the "polymer-multiwall carbon nanotube" composites and composite nanocoatings on macroporous silicon structures.

Influence of sp^3 hybridization bonds on polymer crystallization and strengthening was investigated in composite films. Intensive IR absorption maxima were measured after formation of the "PEI-CNT" composite in the area of the sp^3 hybridization (D) bonds at the frequency of N-H(1) oscillations in the primary amino groups of PEIs. In addition, high IR absorption at frequencies of sp^3 hybridization bonds of polypropylene, polyamide-6 and polyamide-12 with CNTs is determined by $\gamma_\omega(CH)$ and $\gamma_\omega(CH_2)$ vibrations as a result of C-C tetrahedron formation. The IR absorption peak dependencies on CNT content at frequencies of sp^3 hybridization bonds are described by a 1D Gaussian curve for the diffusion equation in the electric field. The electric field intensity between nanotubes and polymer matrix is equal to $6.3 \cdot 10^3$ V/cm at 0.25% CNT. Thus, the way to improve the strength properties of "polymer-CNT" composites is the composite crystallization supported by $\gamma_\omega(CH)$ and $\gamma_\omega(CH_2)$ vibrations in the intrinsic electric field.

The effects of blooming, surface bond passivation and photoluminescence increase were evaluated on macroporous silicon structures with composite nanocoatings. The "PEI-CNT" nanocoatings reduce IR absorption of macroporous silicon with microporous layer by 2-3 orders of magnitude (the blooming effect) due to strong change of band bending on the macropore surface from accumulation one to flat or depleted due to surface bond passivation by composite nanocoating. The photoluminescence intensity of "PEI-CNT" on substrate of macroporous silicon with microporous layer is 5.6 times higher than that of single crystalline silicon. It is due to decrease of the proton non-radiative recombination on the "PEI-CNT" boundary and microporous layer with positive charge of hydrogen atoms.

Acknowledgements

This work was supported by the Project of Scientific and Technical Cooperation between the National Academy of Sciences of Ukraine and the Ningbo University of Technology (China).

References

[1] M. M. J. Treacy, T. W. Ebbesen, and J. M. Gibson, Exceptionally high Young's modulus observed for individual carbon nanotubes, Nature, Vol. 381, 1996, pp. 678-680.
[2] L. Bokobza, Multiwall carbon nanotube elastomeric composites: A review, Polymer, Vol. 48, 2007, pp. 4907- 4920.
[3] W. Bauhofer, and J. Z. Kovacs, A review and analysis of electrical percolation in carbon nanotube polymer composites, Composites Science and Technology, Vol. 69, 2009, pp. 1486-1498.
[4] L. Lacerda, A. Bianco, M. Prato, and K. Kostarelos, Carbon nanotubes as nanomedicines: from toxicology to pharmacology, Advanced Drug Delivery Reviews, Vol. 58, 2006, pp.1460–1470.

[5] J. W. G. Wilder, L. C. Venema, A. G. Rinzler, R. E. Smalley, and C. Dekker, Electronic structure of atomically resolved carbon nanotubes, Nature, Vol. 391, 1998, pp. 59–62.
[6] S. S. Fan, M. G. Chapline, N. R. Franklin, T. W. Tombler, A. M. Cassell, and H. J. Dai, Self-oriented regular arrays of carbon nanotubes and their field emission properties, Science, Vol. 283, 1999, pp. 512–514.
[7] B. Q. Wei, R. Vajtai, and P. M. Ajayan, Reliability and current carrying capacity of carbon nanotubes, Applied Physics Letters, Vol. 79, 2001, pp. 1172–1174.
[8] G. Zou, H. Yang, M. Jain, H. Zhou, D. Williams, M. Zhou, T. McCleskey, A. Burrell, and Q. Jia, Vertical connection of carbon nanotubes to silicon at room temperature using a chemical route, Carbon, Vol. 47, 2009, pp. 933-937.
[9] A. Glushko, and L. Karachevtseva, Photonic band structure of oxidized macroporous silicon, Opto-Electronics Review, Vol. 14, 2006, pp. 201-203.
[10] L. Karachevtseva, S. Kuchmii, O. Lytvynenko, F. Sizov, O. Stronska, and A. Stroyuk, Oscillations of light absorption in 2D macroporous silicon structures with surface nanocoatings, Applied Surface Science, Vol. 257, 2011, pp. 3331-3335.
[11] L. Karachevtseva, Yu. Goltviansky, O. Kolesnyk, O. Lytvynenko, and O. Stronska, Wannier-Stark effect and electron-phonon interaction in macroporous silicon structures with SiO_2 nanocoatings, Opto-Electronics Review, Vol. 22, 2014, pp. 201-206.
[12] L. Karachevtseva, V. Onyshchenko, and A. Sachenko, Photocarrier transport in 2D macroporous silicon structures, Opto-Electronics Review, Vol. 18, 2010, pp. 394–399.
[13] M. Archer, Macroporous silicon electrical sensor for DNA hybridization detection, Biomedical Microdevices, Vol. 6, 2004, pp. 203–211.
[14] Y. Wang, A capacitive humidity sensor based on ordered macroporous silicon with thin film surface coating, Sensors and Actuators B, Vol. 149, 2010, pp. 136–142.
[15] M. Ernst, R. Brendel, R. Ferré, and N.-P. Harder, Thin macroporous silicon heterojunction solar cells, Physica Status Solidi, RRL 6, 2012, pp. 187–189.
[16] P. Panek, Effect of macroporous silicon layer on opto-electrical parameter of multicrystalline solar cell, Opto-electronics Review, Vol. 12, 2004, pp. 45–48.
[17] K. Awasthi, A. Srivastava, and O. N. Srivastava, Synthesis of Carbon Nanotubes, Journal of Nanoscience and Nanotechnology, Vol. 5, 2005, pp. 1616-1636.
[18] V. Lehman, The Physics of Macropore Formation in Low Doped n-Type Silicon, Journal of Electrochemical Society, Vol. 140, 1993, pp. 2836-2843.
[19] L. A. Karachevtseva, O. A. Litvinenko, and E. A. Malovichko, Stabilization of electrochemical formation of macropores in *n*-Si, Theoretical and Experimental Chemistry, Vol. 34, No. 5, 1998, pp. 287-291.
[20] V. F. Onyshchenko , and L. A. Karachevtseva, Conductivity and photoconductivity of two-dimensional macroporous silicon structures, Ukrainian Journal of Physics, Vol. 58, No. 9, 2013, pp. 846–852. http://nbuv.gov.ua/UJRN/Ukjourph_2013_58_9_7
[21] N. M. Resanova, M. T. Kartel, Yu. I. Sementsov, G. P. Prikhod'ko, I. A. Melnik, and M. V. Tsebrenko, Rheological Properties of Molten Mixtures of Polypropylene / Copolyamide / Carbon Nanotubes, Chemistry, Physics and Technology of Surface, Vol. 2, 2011, pp. 451-455. https://www.cpts.com.ua/index.php/cpts/article/view/132
[22] A. M. Berezhkovskii, and A. A. Ovchinnikov, Real width of electron levels in crystal in a constant electric field, Fizika tverdogo tela *(in Russian*), Vol.18, 1976, pp. 3273-3278.
[23] A. M. Berezhkovskii, and A. A. Ovchinnikov, Influence of impurities on the Wannier-Stark ladder in semiconductor in a strong electric field, Physica Status Solidi B, Vol. 110, 1982, pp. 455-459.
[24] M. E. Kompan, and I. G. Aksyanov, Near-UV narrow-band luminescence of polyethylene and polytetrafluoroethylene, Physics of the Solid State, Vol. 51, No. 5, 2009, pp. 1083-1086.

Authors:

1) Liudmyla Karachevtseva, Dr. Sci. (Techn.), Head of the Department of Semiconductor Photonic Structures of V. Lashkaryov Institute of Semiconductor Physics of the National Academy of Sciences of Ukraine. The head of the several researches in the field of semiconductor physics, in particular, semiconductor nanotechnology, which are carrying out in the National Academy of Sciences of Ukraine.

2) Mykola Kartel, Dr. Sci. (Chem.), Prof., Academician, Director of the Chuiko Institute of Surface Chemistry of the National Academy of Sciences of Ukraine. The head of the several researches in the field of physical chemistry, in particular, surface chemistry and physics, which are carrying out in the National Academy of Sciences of Ukraine.

3) Wang Bo, Assoc. Prof., PhD (Econ.), Director of China-Central and Eastern Europe International Science and Technology Achievement Transfer Center of Ningbo University of Technology, Ningbo, China.

4) Yurii Sementsov, PhD (Phys. & Math.), Senior Researcher of Physics and Chemistry of Surfaces, Senior Researcher of the Department of Physical Chemistry of Nanoporous and Nanoscale Carbon Materials of the Chuiko Institute of Surface Chemistry of the National Academy of Sciences of Ukraine. He is an expert in the field of nanosized carbon materials with a graphite-like structure and head of the Project from Ukrainian side.

5) Vyacheslav Trachevskiy, PhD (Chem.), Associate Prof. of the National Aviation University in Kiev. He is an expert in the field polymer materials, composite materials, methods of their preparation and testing.

6) Oleg Lytvynenko, PhD (Techn.), Senior Researcher of the Department of Semiconductor Photonic Structures of V. Lashkaryov Institute of Semiconductor Physics of the National Academy of Sciences of Ukraine. He is an expert in the field of nanosized semiconductor materials, in particular, semiconductor nanotechnology of macroporous silicon.

7) Volodymyr Onyshchenko, PhD (Phys. & Math.), Senior Researcher of the Department of Semiconductor Photonic Structures of V. Lashkaryov Institute of Semiconductor Physics of the National Academy of Sciences of Ukraine. He is an expert in the field of nanosized semiconductor materials, in particular, nonequilibrium processes in semiconductors.